Mon. Not. R. Astron. Soc. **000**, 1–15 (2014) Printed 22 May 2015 (MN LATEX style file v2.2)

Mid-infrared spectroscopy of SVS13: Silicates, quartz and SiC in a protoplanetary disc⋆

Takuya Fujiyoshi[1]†, Christopher M. Wright[2] & Toby J. T. Moore[3]
[1]*Subaru Telescope, National Astronomical Observatory of Japan, National Institutes of Natural Sciences, 650 North A'ohoku Place, Hilo, HI 96720, USA*
[2]*School of Physical, Environmental and Mathematical Sciences, UNSW Canberra, Canberra ACT 2600, Australia*
[3]*Astrophysics Research Institute, Liverpool John Moores University, IC2, Liverpool Science Park, 146 Brownlow Hill, Liverpool L3 5RF*

Accepted 2014 ??? ??. Received 2014 ??? ??; in original form 2014 ??? ??

ABSTRACT

We present *N*-band (8−13 μm) spectroscopic observations of the low-mass, embedded pre-main-sequence close binary system SVS13. Absorption features are clearly detected which are attributable to amorphous silicates, crystalline forsterite, crystalline enstatite and annealed SiO_2. Most intriguingly, a major component of the dust in the envelope or disc around SVS13 appears to be SiC, required to model adequately both the total intensity and polarisation spectra. Silicon carbide is a species previously detected only in the spectra of C-rich evolved star atmospheres, wherein it is a dust condensate. It has not been unambiguously identified in the interstellar medium, and never before in a molecular cloud, let alone in close proximity to a forming star. Yet pre-Solar grains of SiC have been identified in meteorites, possibly suggesting an interesting parallel between SVS13 and our own Solar-System evolution. The uniqueness of the spectrum suggests that we are either catching SVS13 in a short-lived evolutionary phase and/or that there is something special about SVS13 itself that makes it rare amongst young stars. We speculate on the physical origin of the respective dust species and why they are all simultaneously present toward SVS13. Two scenarios are presented: a disc-instability-induced fragmentation, with subsequent localised heating and orbital evolution firstly annealing initially amorphous silicates and then dispersing their crystalline products throughout a circumstellar disc; and a newly discovered shock-heating mechanism at the interface between the circumstellar and circumbinary discs providing the crystallisation process. One or both of these mechanisms acting on carbon-rich grain material can also feasibly produce the SiC signature.

Key words: stars: formation – stars: individual (SVS13) – stars: variables: T Tauri, Herbig Ae/Be – ISM: dust.

1 INTRODUCTION

The Nebular Hypothesis, first formulated separately in the 18th century by Swedenborg, Kant and Laplace, has stood the test of time and is the generally favoured overall description of how the Solar System formed and evolved. In the young hot gaseous nebula, micron-sized dust grains are dragged by the gas, and when they collide they stick with one another and grow in size by forming fluffy or porous aggregates (e.g., Weidenschilling 2000; Poppe 2003). Although the details are still being worked out (see e.g., Chiang & Youdin 2010), those aggregates continue to grow by collision until they become $\gtrsim 1$ km in size (now called planetesimals), at which stage gravity takes over and finally 'runaway' growth of a few bodies leads to planet formation (Weidenschilling 2000; Chiang & Youdin 2010). It is therefore of great interest to study the mineralogy of circumstellar dust around young stars as it represents the original constituents of planetesimals and hence of the rocky planets like our own Earth.

SVS13 (star number 13 in Strom, Vrba & Strom 1976) is a pre-main-sequence (PMS) star (Aspin 2003) thought to be driving the Herbig-Haro objects 7−11 (Bachiller et al. 1998) near the reflection nebula NGC1333 in the Perseus molecular cloud. The bolometric luminosity is estimated to be ∼52 $L_\odot$ (Molinari, Liseau & Lorenzetti 1993; their estimate of 115 $L_\odot$ at 350 pc scaled to an updated distance of 235 ± 18 pc, Horita et al. 2008). Its optical and infrared brightnesses increased considerably sometime between 1988 December and 1990 September (Eislöffel et al. 1991). The brightening was wavelength dependent, with the object becoming bluer as it underwent the change. Even after this period of relatively large increase in brightness ($\Delta m_V \sim 3.3$ mag, $\Delta m_K \sim 1.2$ mag, Eislöffel et al. 1991), SVS13 showed a quasi-periodic near-infrared (NIR) brightness fluctuation with am-

⋆ Based on data collected at Subaru Telescope, which is operated by the National Astronomical Observatory of Japan.
† E-mail: tak@subaru.naoj.org

plitude ∼0.5 mag and cycle ∼500 days between 1990 October and 1993 December (Aspin & Sandell 1994).

The 2.3-μm CO overtone band-heads, indicative of the presence of hot (∼3,000 K) and dense ($\geqslant 10^{10}$ cm^{-3}) molecular gas (Carr, Tokunaga & Najita 2004), probably in the shape of a circumstellar disc, have been observed in emission (Carr 1989; Eislöffel et al. 1991; Biscaya et al. 1997; Carr et al. 2004). The CO band emission also displayed variability on timescales as short as days (Biscaya et al. 1997).

SVS13 is associated with a centimetre source (VLA 4, Rodríguez, Anglada & Curiel 1997) which has been resolved into a close binary (VLA 4A & VLA 4B) separated by ∼0.3 arcsec, first at 3.6 cm (Anglada, Rodríguez & Torrelles 2000) then at 7 mm (Anglada et al. 2004). Although VLA 4A and 4B exhibit similar flux densities at centimetre wavelengths, VLA 4B is the dominant object (by a factor of more than 2) in the millimetre range with its spectral index at these radio wavelengths most probably arising from thermal dust emission (Anglada et al. 2004). The optical/NIR source SVS13 has been associated with VLA 4A by these authors based on older optical data; however, recently Hodapp & Chini (2014) identified SVS13 with VLA 4B, this time using the newer and more (both photometrically and astrometrically) accurate 2MASS catalogue (also, the epoch of the 2MASS observations happens to fall between the epochs of the two radio measurements that discovered and then confirmed the close binary). The separation (∼0.3 arcsec), at the assumed distance to the object of 235 pc, translates to 71 au, or slightly outside the Kuiper Belt in our Solar System.

The first published mid-infrared (MIR) photometry of SVS13 was conducted pre-outburst (Cohen & Schwartz 1983; Harvey, Wilking & Joy 1984). A decade later, without the knowledge of the brightening, Liseau, Lorenzetti & Molinari (1992) obtained 10-μm measurements but did not find the difference (from 10 years before) substantial. The first *N*-band (8–13 μm) spectroscopy (in fact, spectro-polarimetry) of the object was performed by Aitken et al. (1993), using the UCL spectro-polarimeter on the 3.8-m UKIRT with an effective beam diameter of 4.3 arcsec and spectral resolution $R \sim 40$. They remarked that the polarisation spectrum of SVS13 is 'unusual', in that it peaked between 11 and 12 μm, not at the characteristic wavelength of 10.2 μm for silicate grains. Nevertheless, they considered the polarisation to arise from dichroic absorption, albeit by an unusual composition. Wright et al. (1999) re-analysed the same data-set from Aitken et al. (1993), publishing the 'unusual' spectrum for the first time (see also Smith et al. 2000). They concluded that the double-trough-shaped intensity spectrum and the unique polarisation spectrum can only be satisfactorily modelled using inclusions of SiC in an amorphous silicate matrix (this point will be discussed in detail in §4.1.2.1).

In this paper, we present the results of new *N*-band spectroscopic observations of SVS13. The dust mineralogy in the circumstellar environment is investigated by fitting various dust emissivities to the spectrum (§3.2). We also discuss dust components that comprise the best-fit model (§4.1) and suggest their possible origins (§4.2).

2 OBSERVATIONS AND DATA REDUCTION

Table 1 summarises the observations of SVS13 and the standard star HD20644. All measurements were made using the MIR imaging spectrometer COMICS (Kataza et al. 2000) at the Cassegrain focus of the 8.2-m Subaru Telescope on Mauna Kea, Hawaii. The *N*-band low spectral resolution ($R \sim 250$) mode of COMICS utilises two Raytheon 320×240 Si:As IBC arrays, one as a slit-viewer and the other spectrometer, and both are cooled by a Sumitomo 4-K Gifford-McMahon-type cryo-cooler but usually operate at around 7∼8 K because of the self-heating. We used a 2-pixel wide slit to achieve the spectral resolution of $R \sim 250$ in the *N*-band. The pixel scale of the spectrometer in the spatial dimension is 0.165 arcsec so the slit width translates to 0.33 arcsec, which is comparable to the diffraction-limited image size at 10 μm at 8-m class telescopes.

Data reduction was carried out using the IRAF[1] data reduction and analysis package. The chop-subtracted 2-D spectra were flat-fielded and then geometry distortion corrected. Wavelength calibration was achieved using numerous telluric emission lines present in the *N*-band. For flux calibration and telluric absorption correction, we also observed a Cohen standard star HD20644 (Cohen et al. 1999). We furthermore imaged both the target and standard in three different bands (λ_0 = 8.8, 11.7, and 12.4 μm) to rectify possible slit efficiency discrepancy. The images of SVS13 and HD20644, in terms of their point-spread functions, were very similar to each other at all three bands [i.e., SVS13 is unresolved. Indeed, when observing in the spectroscopy mode, the slit was set to run East-West (instrument PA = 90°) in an unsuccessful attempt to resolve the close binary]. In fact, both sets of images of the target and the standard at longer wavelengths, i.e., at 11.7 and 12.4 μm, at which they are even less susceptible to seeing because of its $\lambda^{-\frac{1}{5}}$ wavelength dependence, show the first Airy disc, a clear sign of the diffraction-limited condition. We therefore conclude that only one star (VLA 4B) in the close binary system has any MIR emission associated with it. Hodapp & Chini (2014) could also only find a single object in their laser-guided adaptive-optics assisted *H*- and *K*-band images. As such, in the final stages of the data reduction, three pixels in the spatial direction were simply summed up (i.e., $3 \times 0.165 \sim 0.5$ arcsec) to improve the signal-to-noise ratio.

3 RESULTS AND MODEL FITTING

3.1 Spectrum

Figure 1 shows the COMICS *N*-band spectrum of SVS13. Note that error-bars only represent the standard deviation in the sky background and not the uncertainty in the absolute flux calibration, which would probably amount to about 10 per cent (most of which, approximately 4 to 7 per cent, originates from the uncertainty in the Cohen flux standard template at these wavelengths).

The double-trough shape described in the Introduction is clearly apparent; however, at the spectral resolution $R \sim 250$, it remarkably becomes a triple-trough, with a hump at around 9.5 μm. The first general dip is most likely caused by the silicate absorption, while the second, with its deepest part at about 11 μm, could be due to the presence of SiC, as argued by Wright et al. (1999). The highest spectral resolution so far attained on the object by COMICS, compared to the relatively low resolution of UCLS [$R \sim 40$, see fig.3(b) in Wright et al. (1999) and fig.2.4 in Smith et al. (2000)], displays finer details not previously seen, which will be utilised below for model fitting.

[1] IRAF is distributed by the National Optical Astronomy Observatories, which are operated by the Association of Universities for Research in Astronomy, Inc., under cooperative agreement with the National Science Foundation.

Table 1. COMICS observation log of SVS13 and the standard star HD20644. Integration is the total on-source integration time in seconds, and PA is position angle of slit in degrees, measured East of North.

Date (UT)	Object	Band	Integration (sec)	PA (°)	Airmass
		Spectroscopy			
2009/11/03	SVS13	*N*	994	90	1.224→2.125
	HD20644	*N*	65	0	1.072→2.659
		Imaging			
2009/11/03	SVS13	N8.8	401	–	1.081→1.092
		N11.7	401	–	1.102→1.113
		N12.4	401	–	1.149→1.163
	HD20644	N8.8	22	–	1.059
		N11.7	21	–	1.038
		N12.4	21	–	1.047

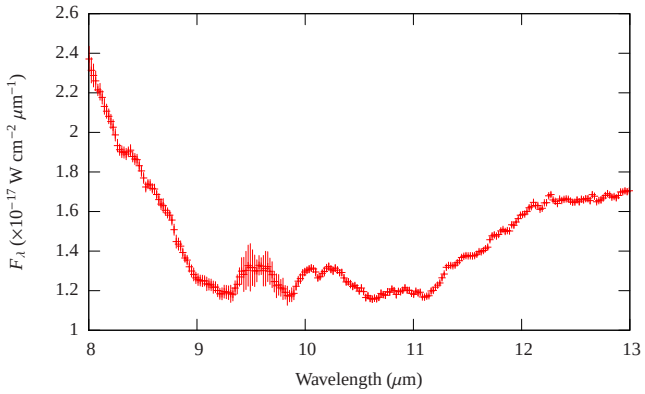

Figure 1. COMICS *N*-band spectrum of SVS13. Note that error-bars only represent standard deviation in the sky background.

3.2 Model fitting

3.2.1 Dust species

Selecting dust species can be subjective exercise but is constrained by those historically identified in astronomical spectra or as (pre-Solar) components of meteorites and interplanetary dust particles. We therefore restrict ourselves in using the following dust species and their combinations.

(i) *Amorphous (astronomical) silicates* (as represented by the Trapezium emissivity, Forrest, Gillett & Stein 1975). Although their specific mineralogy has been extremely difficult to identify, they are the most abundant dust grains in the interstellar medium (ISM; e.g., Molster, Waters & Kemper 2010). The emissivity has been derived by dividing the observed *N*-band spectrum of the Trapezium region (Forrest et al. 1975) by a 250-K Planck black-body function (Gillett et al. 1975).

(ii) *SiC* (carbon star emissivity, Aitken et al. 1979). It is a major component in carbon-rich stellar ejecta (e.g., Treffers & Cohen 1974) and is also found in meteorites as pre-Solar (probable extra-Solar-System) grains (e.g., Bernatowicz et al. 1987); however, it has never been observed in the ISM (Whittet, Duley & Martin 1990). We note that, using an Infrared Space Observatory (*ISO*) SWS spectrum, a later study (Min et al. 2007) has found some evidence of the existence of SiC grains in the *N*-band 'ISM' absorption feature in the line of sight towards the Galactic Centre (GC) source Sgr A*; however, the large beam size (14×20 arcsec^2) of *ISO* encompasses a number of asymptotic giant stars (i.e., the most probable source of meteoritic SiC grains, e.g., Zinner 1998) identified in several catalogues (Blum, Sellgren & Depoy 1996; Ott, Eckart & Genzel 1999; Clénet et al. 2001; Blum et al. 2003). We therefore suspect it may be contaminated and so may not represent the pure ISM extinction. Whittet et al. (1990) studied *N*-band spectra of 10 GC sources from Roche & Aitken (1985), which were obtained using the UCL spectrometer with a moderate beam diameter of 4.2 or 4.3 arcsec, thus those data should be less susceptible to contamination by source confusion. Regardless of its existence in the ISM, it has never been detected in the circumstellar environment of young stars.[2] The emissivity has been derived by dividing the observed *N*-band spectrum of the carbon star Y-Tau by a 800-K Planck black-body function (Aitken et al. 1979).

(iii) *Crystalline silicates* (aerosol forsterite and enstatite, Tamanai et al. 2006). The *ISO* 'crystalline silicate revolution' revealed they are frequently present in stars young and old (Jäger et al. 1998). Now, *Spitzer* has both expanded and refined the crystalline silicate database (e.g., Olofsson et al. 2009); however, once again, they have never been identified in the diffuse ISM (Kemper, Vriend & Tielens 2004) [a caveat here is that the work of Min et al. (2007) mentioned above used the same dataset from Kemper et al. (2004), i.e., the *ISO* SWS spectrum of the GC source Sgr A*, which may not describe the true nature of the ISM dust grains]. The two most abundant crystalline silicate species are forsterite (Mg_2SiO_4) and enstatite ($MgSiO_3$, Molster et al. 2010). Commercially available crystalline silicate dust powders were dispersed into a nitrogen gas stream to create non-embedded, free-flying particle samples for infrared extinction measurements (Tamanai et al. 2006).

(iv) *Amorphous and annealed SiO_2* (Fabian et al. 2000). It is one of the most abundant compounds in the Earth's crust but its features have not been observed in the diffuse ISM (see e.g., Li & Draine 2002). It has however been identified in a number of protoplanetary discs around young stars (e.g., Sargent et al. 2009a). For the crystalline component, we use the nano-particles of precipitated silica annealed at 1,220 K for 5 hours (Fabian et al. 2000).

[2] An over-abundance of carbon has been reported in the debris disc of the archetypal young star β-Pictoris (Roberge et al. 2006). Although SiC is not explicitly referred to, it may be posited that one of the most likely compounds which could form in such a carbon-rich atmosphere is silicon carbide.

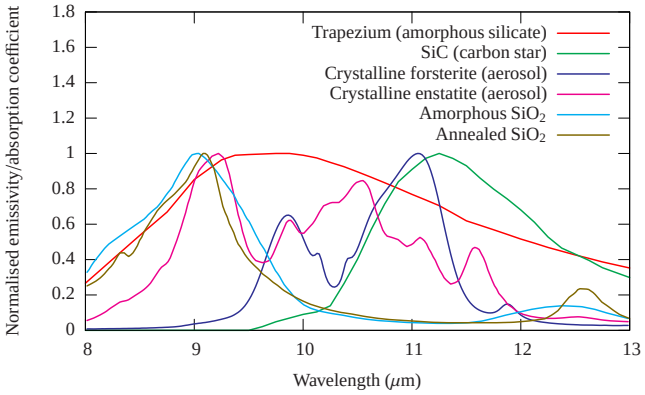

Figure 2. Normalised emissivities/absorption coefficients of the selected dust species (see text).

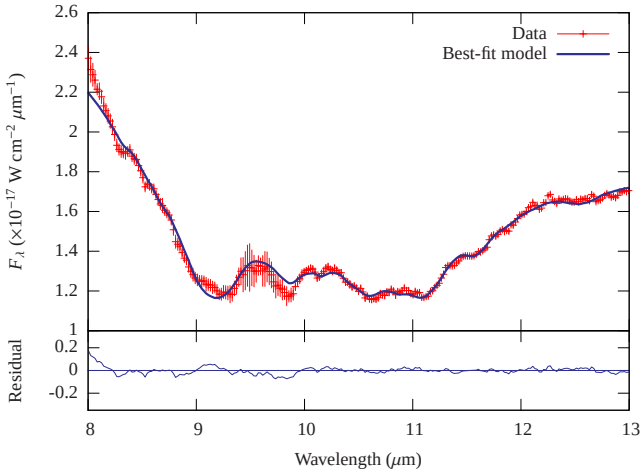

Figure 3. *Upper panel*: *N*-band spectrum of SVS13 overlaid with the best-fit model (solid line). *Lower panel*: Fitting residual plot.

We use either empirical (amorphous silicates and SiC) or experimental (crystalline silicates and amorphous/annealed SiO_2) results on an ensemble of presumably differently shaped/sized grains. This approach is slightly varied from a number of other mineralogical studies which usually adopt some optical constants and shape distributions to calculate absorption coefficients (e.g., Bohren & Huffman 1983). It is unrealistic to expect dust grains to have regular shapes and indeed a sample of interplanetary particles consists of irregularly shaped porous aggregates (see e.g., Bradley 2003). Also, SVS13 is polarised in the MIR (i.e., aligned aspherical grains must be present, Aitken et al. 1993), hence we consider our approach to be at least a more pragmatic one. Normalised emissivities/absorption coefficients of the materials used in this study are shown in Figure 2.

3.2.2 *Model*

The fitting function can be expressed as

$$F_\lambda \propto B_\lambda(T) \times e^{-\alpha}$$

where $B_\lambda(T)$ is the Planck black-body function at temperature T, $\alpha = \sum_{i=1}^{k} \tau_i$ is the total optical depth of k absorption components and τ_i is the optical depth of each component. In order to keep the fitting as simple as possible, we did not consider, for example, an extra black-body component, self-absorption of a dust species, etc.

We used an IRAF task *specfit* (Kriss 1994) to fit the emissivities/absorption coefficients. The fitting results are summarised in Table 2. As the Planck black-body function is always present, we distinguish between each model with the number of absorption components (k-comp, where k is the number of different dust species) and the names of specific absorptive ingredients added [am and cr stand for amorphous and crystalline, and Trap Trapezium (amorphous/astronomical silicates), fors/fo forsterite, enst/en enstatite, respectively. Every model is also given a unique alphabetical identification index (A–I), as listed at the beginning of each row].

The goodness of fit is given by the reduced chi-square, $\chi^2_\nu \equiv \chi^2/\nu$, where ν is the number of degrees of freedom. Since there is only one emissive component (a black-body) and the rest are always absorptive, which all naturally come after the black-body, the order in which the absorptive components appear should not matter (i.e., they are commutative). We have indeed obtained exactly the same results (minimum χ^2_ν and τ values) even when the order in the component list was altered. It is interesting to note that when the SiC (*plus* Trapezium) emissivity is combined with only one of the crystalline silicate species (forsterite or enstatite), their best-fit parameter values are rather uncertain [by more than 10 per cent; see models C (2-comp+cr fors) and D (2-comp+cr enst) in Table 2]; however, when all three (SiC, crystalline forsterite and enstatite, *plus* Trapezium) are combined, their best-fit values become significantly more certain [by $\leqslant$ 5 per cent; see model E (2-comp+cr fo&en)]. This is most probably a manifestation of the fact that it takes all three emissivities/absorption coefficients to fit well the complex spectral shape longward of ∼10 μm.

The general trend is clearly such that the more components there are, the better the fit, as one might expect. However, it stops when both amorphous and annealed SiO_2 are added to the mix. Were the trend to continue, one would have expected to obtain the smallest χ^2_ν for the combination that involves all the dust species considered in this study. Not only did χ^2_ν not improve but also the contribution from amorphous SiO_2 became insignificant (in addition, its best-fit τ is poorly constrained, with the associated uncertainty at nearly 30 per cent, while all the other values show reasonable certainty at well below 10 per cent). Combining these findings with the fact that adding annealed SiO_2 alone gives a better fit than the amorphous counterpart in its place, we consider model G (4-comp+cr SiO_2, i.e., a black-body, amorphous silicates, SiC, crystalline forsterite and enstatite, plus annealed SiO_2) the best-fit model with the fewest number of components. Figure 3 shows the *N*-band spectrum of SVS13 overlaid with the best-fit model (solid line).

The model's ability to reproduce fine structures, especially the longward of ∼10 μm, is remarkable, considering the complexity of the spectrum. The only obvious shortcomings of the model prediction are: the slightly shallower slope towards the short-end of the *N*-band window; not reproducing well the shape of the 8.3-μm absorption feature; the slightly deeper absorption at about 9.1 μm; slightly shallower absorption at around 9.8 μm; not predicting adequately the sharpness of the 10.1-μm absorption signature, et cetera (see also the fitting residual plot in the lower panel of Figure 3). However, it has been known for some time that, for laboratory measured absorption spectra of dust species, the method of preparation of dust samples is critically important. For example, hand-grinding and ball-milling will produce different results (Koike et al. 2010). Annealing processes (at different temperatures and for different durations) also affect the outcome and depending on the treatment, peak positions and full-widths at half-maximum

Table 2. *specfit* results of various model fitting (see text for details). In Column 1, alphabetical model IDs and names of various models discussed in the text are listed. The goodness of fit, χ^2_ν, is given in Column 2. In Columns 3, the black-body temperature (in K) is given. In Columns 4–15, optical depths of each dust component and their associated uncertainties (given by *specfit*, converted to per cent) are listed.

	Model	χ^2_ν	$T(K)$	Trap	err	SiC	err	Cr fo	err	Cr en	err	Am SiO_2	err	Cr SiO_2	err
A	1-comp	30.0	319	1.11	2%										
B	2-comp	10.5	298	0.94	1%	0.18	4%								
C	2-comp+cr fors	8.33	300	0.86	1%	0.14	13%	0.08	34%						
D	2-comp+cr enst	6.51	301	0.66	4%	0.18	13%			0.23	13%				
E	2-comp+cr fo&en	3.74	302	0.55	2%	0.15	4%	0.10	5%	0.24	1%				
F	4-comp+am SiO_2	1.95	313	0.56	<1%	0.17	2%	0.12	4%	0.24	2%	0.15	6%		
G	4-comp+cr SiO_2	1.67	309	0.60	1%	0.18	3%	0.11	5%	0.21	5%			0.16	2%
H	4-comp+am&cr SiO_2	1.67	310	0.59	<1%	0.18	3%	0.11	6%	0.21	3%	0.02	29%	0.14	4%
I	G−SiC	14.7	314	0.56	<1%			0.18	4%	0.23	4%				

of dust features will differ, sometimes significantly (Koike et al. 2010; see also Fabian et al. 2000). When these further complications are taken into account, it is even more impressive how good a fit the selected model components provided, considering the complexity of the features modelled and the limited number of dust species required. In the following discussion, we assume that the dust components present in the best-fit model exist in the circumstellar environment of the PMS star SVS13.

4 DISCUSSION

4.1 Dust species (revisited)

4.1.1 Amorphous (astronomical) silicates

As mentioned earlier, they are the most abundant dust species in the diffuse ISM (Molster et al. 2010). The broad, smooth absorption feature arising from the Si−O stretching mode, peaking at about 9.7 μm, is the strongest and best studied infrared feature in the diffuse ISM (e.g., Whittet 2003), although identifying their specific mineralogy or composition has traditionally been extremely difficult, especially if accompanying 20-μm data is not available. Most, if not all, astronomical mineralogy studies contain amorphous silicates in one form or another (see, for example, tab.1 in Molster et al. 2010). Therefore, it is not surprising that the amorphous silicate absorption appears prominently in the *N*-band spectrum of a young star. However, we do not attempt to associate it with a particular mineral, but rather use a generic representation of amorphous silicates in a star-forming region as provided by the Trapezium emissivity.

4.1.2 SiC

Silicon carbide has never been observed in the diffuse ISM (Whittet et al. 1990), although it is produced in carbon star ejecta and is undoubtedly injected into it. So where does it go? One simple explanation may be that dust grains are destroyed in the ISM by, for example, supernova shock waves (e.g., Jones, Tielens & Hollenbach 1996). If the substantial gap between the dust lifetime ($\sim 10^8$ yr, Jones et al. 1994; 1996) and the dust injection timescale (from dust formation in the outflows of dying stars to being incorporated into new star-forming regions; $\sim 10^9$ yr, Dwek & Scalo 1980; Jones & Tielens 1994) is valid, then SiC grains may also have been destroyed, hence no 11.3-μm SiC feature detected in the ISM. However, as mentioned earlier, pre-Solar SiC grains (and many others) have been found (e.g., in a carbonaceous chondrite Murray by Bernatowicz et al. 1987) so some dust grains must survive the harsh ISM.

SiC has in fact also been suggested as a dust component in a number of comets (Orofino, Blanco & Fonti 1994). Good fits to the *N*-band spectra of three comets (1P/Halley, C/1987 P1 Bradfield, and 1986l Wilson), which all exhibited two broad peaks centred at about 9.7 and 11.3 μm,[3] were obtained using a laboratory measured spectrum of synthetic amorphous olivine (i.e., silicate, Blanco et al. 1991) and the complex refractive index of α-SiC from Pegourie (1988). It should be noted, however, that the 11.3-μm feature in comets has generally been attributed to crystalline silicates (e.g., for Halley's comet, Campins & Ryan 1989). While the available data is limited to the *N*-band spectrum alone, its identification unfortunately remains rather ambiguous as their signatures are often overwhelmed by that of amorphous silicates. Only when measurements at other wavelengths (especially at 20 μm and longer) are on hand, the crystalline silicate assignment becomes more robust (e.g., for Comet Hale-Bopp using the *ISO* SWS data, Crovisier et al. 1996; 1997). Those three comets (and Hale-Bopp also) are all long-period Oort Cloud comets which are thought to have originated just beyond the ice giant formation region ($\gtrsim 15$ au, Charnoz & Morbidelli 2007; Levison et al. 2008).

The most conclusive evidence for the presence of pre-Solar SiC grains in comets came from dust samples, captured and returned to Earth by NASA's Stardust mission to Comet 81P/Wild 2 (Messenger et al. 2009), which belongs to short-period Jupiter Family of comets (JFCs), which are likely to have formed in the Kuiper Belt ($\gtrsim 30$ au). The discovered 300-nm SiC grain is unique, in that it is the only pre-Solar grain so far found in the silica aerogel dust collector, possibly reflecting the complex preparation required for the aerogel track analysis (Floss et al. 2013), and no pre-Solar SiC grains have yet been detected in the impact craters on the surface of exposed aluminium foils. The abundance of pre-Solar SiC grains in 81P/Wild 2 has been estimated to be ∼45 ppm (Floss et al. 2013), which is consistent with that in insoluble organic matter residues from a number of different classes of chondritic meteorites (10−55 ppm, Davidson et al. 2009). These findings reveal that SiC grains must have been available in a wide range of distances from the Sun, from the carbonaceous chondrite formation region of the inner few au to the comet-forming outer reaches of the proto-Solar nebula.

[3] Comet Wilson showed an extra, unidentified emission feature at around 12.5 μm but it was omitted from fitting procedure (Orofino et al. 1994).

Interestingly, pre-Solar SiC grains found in another carbonaceous chondritic meteorite Murchison, for example, showed little evidence of scarring (Bernatowicz et al. 2003) due, for instance, to grain-grain collisions. Were the interstellar environment as destructive as it has been described (e.g., by Jones et al. 1996), such hallmarks should certainly be present. Then again, whether a dust grain survives is probably largely statistical in nature and it is perhaps only natural that those that do show little damage. Nonetheless, when Jones & Nuth (2011) re-examined the dust lifetime using revised uncertainty estimates, they found it to be comparable with the dust injection timescale.

Whittet et al. (1990) proposed an alternative solution to the missing SiC problem: oxidation. They argued that the ejected SiC grains could be selectively destroyed by surface oxidation in the O-rich interstellar environment. Indeed, partial oxide layers on some pristine pre-Solar SiC grains from the Murchison meteorite have been reported (Croat, Stadermann & Bernatowicz 2010a). In volatilisation experiments of SiC grains under Solar nebula-like oxidising conditions (Mendybaev et al. 2002), either continuous or partial SiO_2 layers are formed, depending on oxygen fugacities (continuous at higher and partial at lower fugacities, or more and less oxidising, respectively). Similarly, though probably unintentionally, an oxide layer had grown on the surface of SiC nano-particles after they were taken out of a vacuum chamber (Clément et al. 2003). However, even though a SiO_2 layer does add new features due to the presence of the mantle material, it does not appear to suppress very much the 11.3-μm SiC feature (Posch, Mutschke & Andersen 2004; Zhang, Jiang & Li 2009).

In a similar study to Croat et al. (2010a), Croat, Bernatowicz & Stadermann (2009a) and Croat, Lebsack & Bernatowicz (2010c) identified coatings mainly consisting of carbonaceous material on the surface of some pristine pre-Solar SiC grains also from Murchison. Furthermore, once again from the same meteorite, some graphite spherules were found to contain SiC grains (Bernatowicz et al. 1996; Croat & Stadermann 2006; Hynes, Croat & Bernatowicz 2007; Croat, Stadermann & Bernatowicz 2008; Croat & Stadermann 2008; Croat, Stadermann & Bernatowicz 2010b). Such SiC-containing graphites have also been found in samples from another meteorite, Orgueil (Croat et al. 2009b; Croat, Bernatowicz & Jadhav 2014). The discoveries of these SiC-containing graphites are quite significant as they are clear evidence that pre-Solar SiC grains either formed earlier than or at about the same time as the graphites. One spherule in particular (only one of a kind so far), discovered by Croat & Stadermann (2008), houses a SiC grain at its centre, most probably indicating the central SiC acted as a nucleation core (i.e., SiC may have been formed first). It should be noted, however, that the number of SiC inclusions hitherto found is rather limited; only about a dozen graphite spherules that contain SiC grains have been reported (see references listed above), whilst graphites with internal carbides (predominantly TiC, Croat et al. 2008) number ∼80 to date, despite the fact that the abundance of Ti is very much lower than that of Si.

These results (the scarcity of SiC-containing graphites and much more numerous TiC inclusions) can be explained by a relative condensation sequence of solids in carbon star outflows; in conditions typically found for carbon stars, the condensation sequence is thought to be TiC, graphite, and then SiC (Lodders & Fegley 1995). There have however been some suggestions that, under certain circumstances, SiC is formed before graphite (Chigai & Yamamoto 2003; Yasuda & Kozasa 2012). In fact, condensation in this order (SiC before graphite) has been invoked to account for the lack of the 11.3-μm SiC feature in the diffuse ISM (Frenklach, Carmer & Feigelson 1989; Kozasa et al. 1996). As SiC grains formed in the vicinity of carbon-rich stars travel further away and become cooler, a carbon layer develops on the grains and hides the SiC feature. Such scenario was in fact briefly mentioned by Whittet et al. (1990), and unlike the oxide coating discussed earlier, the carbon mantle seems to suppress successfully the 11.3-μm signature (Kozasa et al. 1996; Papoular 2008).

A short letter has been published in a surface science journal that reports the dissolution of the amorphous carbon layer into the SiC core, when the core-mantle grain was heated to 600°C (873.15 K) under high vacuum (3×10^{-8} Torr, Kimura, Saito & Kaito 2003). At 800°C (1,073.15 K), the surface layer completely disappeared without altering the lattice structure of the particle. Somewhat surprisingly, they have further observed that when the SiC grain was cooled back to room temperature, still under high vacuum and thus without any significant contaminants, the amorphous carbon coating re-emerged (i.e., the process is reversible, Y. Kimura et al. 2003). The temperature reached in their experiment (1,073.15 K) is above the glass transition temperature of amorphous analogues of enstatite ($MgSO_3$) composition (1,040 K, Roskosz et al. 2011). As crystalline dust species (crystalline forsterite and enstatite, and annealed SiO_2; see §4.1.3 & 4.1.4) are also present, temperatures reached in the circumstellar environment of SVS13 must have been high enough to produce those and remove the carbon coating from the SiC grains. Under presumably much more severe conditions encountered, the amorphous carbon layer could still be absent from the SiC core even at sufficiently low temperatures ($\lesssim$ 100 K at $\gtrsim$ 15 au, Poteet et al. 2011) for the grains to exhibit the SiC absorption feature. Recall that Wright et al. (1999) concluded that SiC grains are most likely to be included in an amorphous silicate matrix (see also §4.1.2.1).

To our knowledge, it has never been established whether the re-heated SiC particles would exhibit (in absorption) exactly the same feature as that seen towards carbon stars. In any event, it is known to vary somewhat from one carbon star to another; so much so that, Speck, Thompson & Hofmeister (2005) have coined a term '∼11-μm feature' (i.e., with the approximation mark '∼' and fewer significant figures) to emphasise its variability. Also, a self-absorbed SiC band has been detected towards extreme carbon stars (Speck, Barlow & Skinner 1997; Justtanont et al. 1997; Hony, Waters & Tielens 2002), where amorphous carbon might be expected to dominate. Therefore, although this scenario (resurgence of the SiC feature in a warm environment) may plausibly explain the situation in SVS13, it should be treated with caution.

However, we highlight the fact here that if we take out the SiC component from the best-fit model (I ≡ G − SiC = a black-body, amorphous silicates, crystalline forsterite and enstatite),[4] the resulting fitting χ^2_ν value (14.7) is better than that for the most basic model A (1-comp = a black-body plus amorphous silicates; 30.0) but worse even than the one for the simple model B (2-comp = a black-body, amorphous silicates, and SiC; 10.5), signifying need for the SiC inclusion. See Figure 4 which compares models B and I. It is clear, apparent in the residual plot in the lower panel, that the fit

[4] When SiC was taken out of the best-fit model, the contribution from annealed SiO_2 became rather insignificant or even negative (i.e., turned emissive). We have therefore decided to exclude it from the fitting procedure in this test case. The inference drawn in this section would still be valid regardless of the crystalline SiO_2 inclusion.

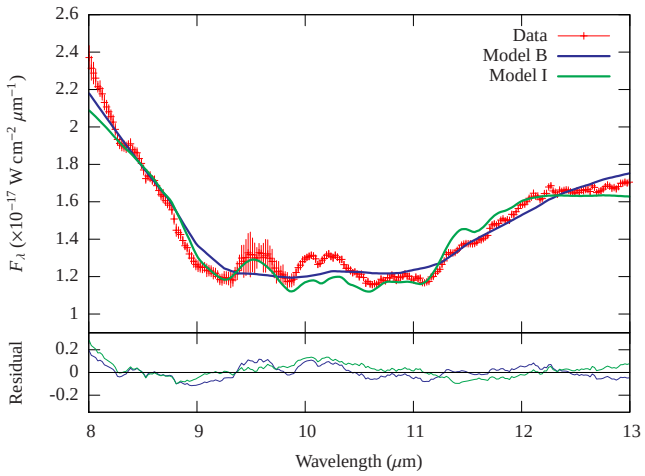

Figure 4. *Upper panel*: *N*-band spectrum of SVS13 overlaid with models B and I. *Lower panel*: Fitting residual plot for the two models.

for model I becomes much worse than that for model B longward of ∼10 μm, especially around 11.3 μm, where the contribution from the SiC emissivity is significant.

4.1.2.1 Polarimetry perspective Similar to the conventional spectrum, the MIR polarisation spectrum of SVS13, first discussed in Wright et al. (1999) and Smith et al. (2000), is perhaps the most unique ever observed (see Figures 5 and 6). Given the peak occurs beyond 11 μm and the overall profile has an approximate 'tilde' shape, properties similar to those predicted for polarised emission (Martin 1975; Aitken 1989), at first glance it is not even obvious whether the spectrum is representative of dichroic absorption or instead polarised emission. Also, that the total flux density spectrum is obviously dominated by absorption does not necessarily imply the polarisation profile would also be indicative of absorption. Instances can occur where the polarisation is dominated by emission but the conventional flux density shows deep absorption, an effect first predicted by Thronson (1979) and seen in a few sources (e.g., NGC7538 IRS1 and RCW57 IRS1 in Smith et al. 2000).

Fortunately in the case of SVS13 there is additional polarisation data in the NIR, up to almost 3.5 μm, which can be compared with the MIR (Holloway et al. 2002 and references therein). Most specifically the measured polarisation position angles in the two spectral regions are almost identical at ∼50 ± 5 degrees. The NIR polarisation is almost certainly due to dichroic absorption since it rises through the 3-μm water-ice band. There can be no polarised emission through this band because the ice would obviously melt at the 500−1,000-K temperatures characteristic of NIR emission (and it is unclear if relevant grain alignment mechanisms could operate at such a high temperature). Thus, given the equality of the position angles, it is very likely that the MIR polarisation is also due to dichroic absorption.

Having established the polarisation process as dichroic absorption it remains to determine what type of dust can produce such a unique 8−13-μm profile, and especially a peak beyond 11 μm. Possible candidate carriers with bands around 11 μm and longer, inferred in other astronomical spectra and/or found within pre-Solar meteoritic grains, include crystalline silicates and SiC, as shown in Figure 2, as well as water ice, Polycyclic Aromatic Hydrocarbons (PAHs), aluminium oxides and carbonates. Polarisation models have been run for all of these potential constituents, either as inclusions mixed in with an amorphous silicate host matrix or as a confocal mantle coating an amorphous silicate core.

Details of the modelling will be presented elsewhere (Wright et al. in preparation), but are based on the Rayleigh approximation for spheroidal particles. At MIR wavelengths, according to Somsikov & Voshchinnikov (1999), this is adequate for grain radii (of an equivalent volume sphere) up to at least 0.5 μm, where the relative difference between exact and Rayleigh solutions is less than 10 per cent for the water ice coated grains of their work. Relevant formulae for the absorption and polarisation cross sections of both bare and mantled spheroids are given in Draine & Lee (1984) and Lee & Draine (1985), whilst those for an 'average' dielectric function of a mixture, using effective medium theory such as the Maxwell-Garnett rule, are provided in Bohren & Huffman (1983). In all cases we have used an oblate core with principal axis ratio of 2, parameters which are reasonably constrained from other observations (e.g., Hildebrand & Dragovan 1995; Draine & Allaf-Akbari 2006).

The amorphous silicate optical constants are those of 'astronomical silicate', first formulated by Draine & Lee (1984), and subsequently updated by Laor & Draine (1993), Weingartner & Draine (2001) and Draine (2003). The MIR component of these optical data sets was constructed to reproduce the spectrum of Trapezium, so our choice is consistent with the emissivity function we used to model the conventional (total flux density) spectrum in §3.2.

As might be expected based on the absorption coefficients shown in Figure 2, polarisation features of crystalline silicates, such as inclusions of the crystalline olivine of Mukai & Koike (1990), are simply too narrow to match the observed SVS13 polarisation spectrum. They instead produce a spectrum which looks much like the polarisation profile of the massive embedded young stellar objects (YSOs) AFGL2591 (Aitken et al. 1988; Wright et al. 1999) and IRAS13481−6124 (Wright et al. 2008), two sources with a sharp polarisation feature at ∼11.2 μm superposed on the much broader amorphous silicate band. Similar comments hold for PAHs and carbonates. Whilst its resonance is relatively broad, aluminium oxide inclusions merely produce a shoulder, or long-wavelength wing, on the amorphous silicate polarisation profile (Wright et al. 2002).

The long-sought but rarely identified 12-μm librational band of water ice, occurring between ∼12 and 13 μm for the crystalline and amorphous phases respectively (Maldoni et al. 1998), may be thought to be a strong candidate. SVS13 does have the characteristic 3.1-μm H_2O ice absorption band, which Parise et al. (2003) note is more like that from crystalline than amorphous ice. Its optical depth however is not particularly high, only around 0.55. This compares to values of around 1 to 3.5 in a sample of embedded YSOs in Smith, Sellgren & Tokunaga (1989). Their study included another source with an unusual 8−13-μm spectrum, namely the eastern component of the double source AFGL961, with a 3.1-μm optical depth of 2.46.

Indeed, the only previous identification of the librational band was made for AFGL961, firstly by Cox (1989) using *IRAS* and then by Smith & Wright (2011) for each component using *Spitzer*. This has recently been questioned by Robinson, Smith & Maldoni (2012) on the basis of radiative transfer models suggesting the 8−13-μm silicate feature could be self-absorbed, leading to a local minimum between the 10- and 20-μm silicate bands occurring around 13 μm and thus mimicking ice absorption. However, their models only do an average job of reproducing the overall shape of the observed 2−20-μm spectrum and profile of the 8−13-μm fea-

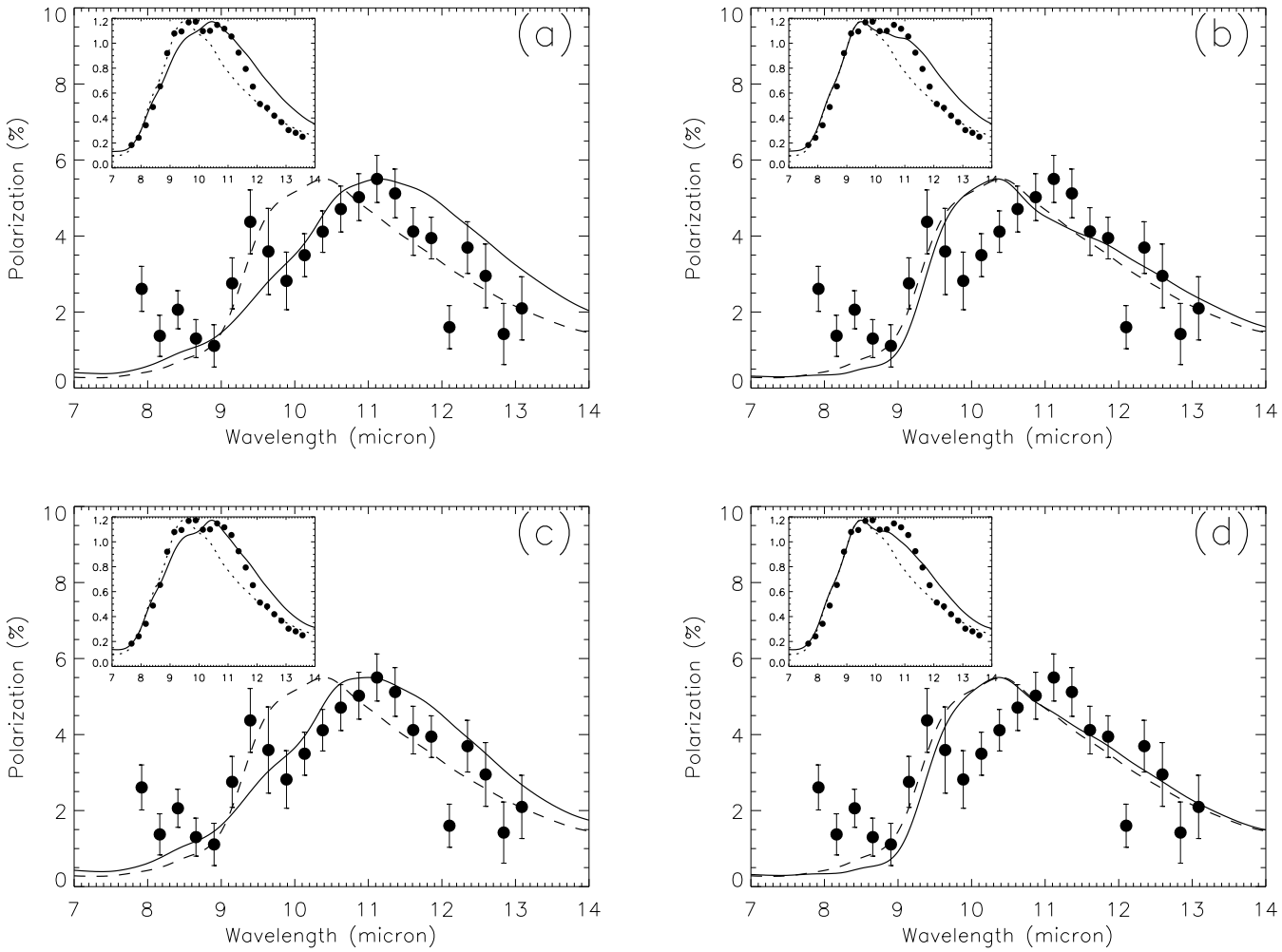

Figure 5. SVS13 polarisation spectrum (solid circles) overlaid with various polarisation models (solid lines) calculated for spheroids in the Rayleigh approximation. The data around 9.5 μm are compromised by telluric ozone. Insets show the optical depth profile extracted from the conventional flux density spectrum. The dashed line in all panels (insets) corresponds to the polarisation (absorption) expected from 'astronomical silicate' of Draine (2003). In (b) and (d) are models with a mantle of amorphous (b) and crystalline (d) water ice, and a mantle-to-core volume ratio of 0.5. Models in (a) and (c) are for silicate-ice mixtures, again using amorphous (a) and crystalline (c) ice with a volume fraction of 0.375 and a Maxwell-Garnett mixing rule for the dielectric function of the effective medium. In all cases the grain cores are oblate with an axial ratio of 2:1.

ture. Also, they only modelled AFGL961E and not AFGL961W, which has a prominent silicate emission feature but still shows the same apparent absorption at 13 μm (as well as CO_2 ice absorption at 15 μm). Whatever the case, as presented in Boogert et al. (2008), there is sufficient evidence that the librational band has been detected toward at least a few YSOs (although none look much like SVS13 itself).

Thus, polarisation models with water ice either as a mantle or as inclusions were attempted. Ice existing as a mantle on silicate cores is the 'standard' model for dust in molecular clouds (e.g., Gibb et al. 2004). On the other hand, the idea behind ice as inclusions is that if silicate grains are initially porous or fluffy, then within a cold molecular cloud (or disc) water ice may condense to fill the pores. Alternatively, ice-mantled grains may collide and stick together, resulting in a similar type of grain structure.

Whatever the case, core-mantle grains cannot produce the position of the polarisation peak in SVS13. See Figure 5, which shows in (b) and (d) models using a mantle of respectively amorphous and crystalline water ice (optical constants from Leger et al. 1983 and Bertie, Labbé & Whalley 1969, respectively). The mantle-to-core volume ratio is 0.5, but in fact mantles do not sufficiently change the overall polarisation profile even up to mantle-to-core volume ratios of 4 or more. The 10.3-μm peak of bare amorphous silicates is still clear, and indeed sharper and higher than the water ice peak around 12 μm, whilst the observed SVS13 peak lies in the trough between them.

On the other hand, as seen in Figure 5 (a) and (c), a silicate-ice mixture can reasonably match at least the overall shape and peak position of the SVS13 polarisation spectrum for an ice-to-silicate volume ratio of 0.375. A serious flaw however is that it predicts large polarisation in the 3-μm water ice band, e.g., an excess of ∼6–8 per cent over the continuum compared to an observed value of $\leqslant$ 1.5 per cent described in Aitken (1996) and Chrysostomou et al. (1996). This assumes that grains are small enough that the Rayleigh approximation remains valid at 3 μm, reasonable for grain sizes $\leqslant$ 0.5 μm. See tab.2 in Somsikov & Voshchinnikov (1999), where the relative difference between exact and Rayleigh solutions only increases to 10–15 per cent at 3 μm for either oblate or prolate grains with an 'equivalent volume' spherical radius of 0.5 μm.

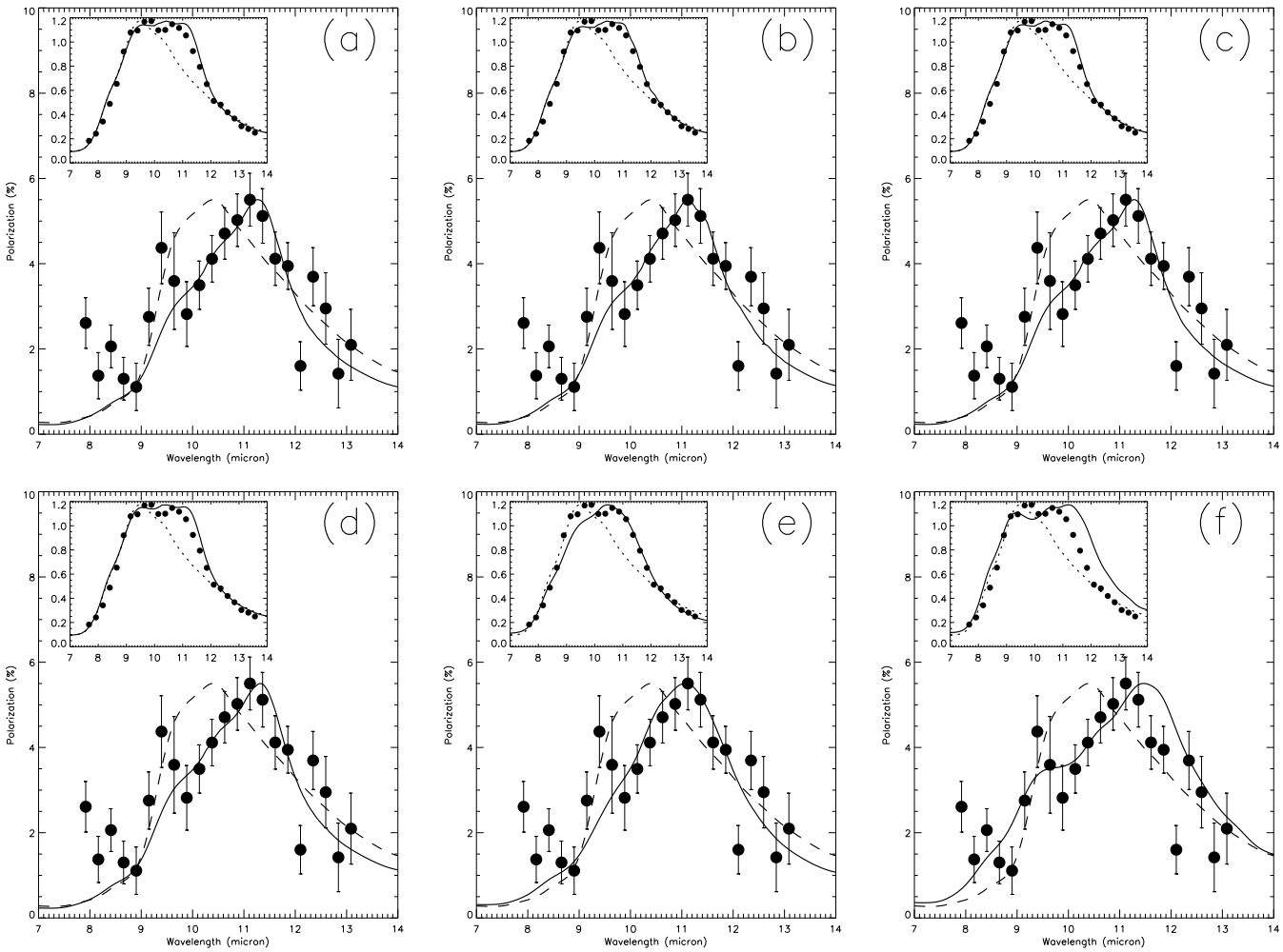

Figure 6. SVS13 polarisation spectrum (solid circles) overlaid with various polarisation models (solid lines) calculated for spheroids in the Rayleigh approximation. The data around 9.5 μm are compromised by telluric ozone. Insets show the optical depth profile extracted from the conventional flux density spectrum. The dashed line in all panels (insets) corresponds to the polarisation (absorption) expected from the Draine (2003) 'astronomical silicate'. Panels (a)−(c) use SiC optical data from Pitman et al. (2008) for cubic (a), hexagonal e-ray (b) and hexagonal o-ray (c) samples. Panel (d) uses α-SiC refractive indices from Choyke & Palik (1985), panel (e) 'astronomical SiC' from Laor & Draine (1993) and panel (f) α-SiC from Pegourie (1988). In all cases the grains are oblate with an axial ratio of 2:1.

Included in each panel of Figure 5 is an inset showing the optical depth extracted from the UCLS spectrum of SVS13 as presented in Smith et al. (2000), compared to the absorption cross section of the respective models. The optical depth was calculated by fitting a Planck function between the short and long wavelength ends of the spectrum, after correcting them for a grey component of emissivity taken to be the Trapezium emissivities at 7.5 and 13.5 μm. The inferred colour temperature is around 350 K, not too dissimilar to the model-based temperatures listed in Table 2. In no case does water ice, either as a mantle or as inclusions, match the optical depth profile. We therefore conclude that water ice is highly unlikely to be responsible for the unique SVS13 MIR spectrum, unless its optical properties are much different to those used here (which are extremely similar to those presented in many other publications).

Thus, the only remaining alternative is SiC and indeed this provides the best match to the observed SVS13 MIR polarisation spectrum. See Figure 6 which shows polarisation models of SiC inclusions within an amorphous silicate matrix, using the Maxwell-Garnett mixing rule to calculate the effective dielectric function. Several different dielectric functions of SiC were trialed, namely: cubic (3C or β) and two samples of hexagonal (6H or α) for E both perpendicular and parallel to the c-axis, derived by Pitman et al. (2008) from single-crystal reflectance spectroscopy; α-SiC in Choyke & Palik (1985), also from reflectivity measurements; an 'astronomical SiC' from Laor & Draine (1993) derived from several different laboratory data sets; α-SiC determined from particle transmission measurements and presented by Pegourie (1988).

All can provide good matches to the overall profile of the observed spectrum, with respective volume fractions of the SiC inclusions of 0.1 for the Pitman et al. and Choyke & Palik data sets, and 0.25 for the Laor & Draine and Pegourie optical data. Whilst the models are all qualitatively similar, apart perhaps from the Pegourie case, the best match appears to be for the 6H (hexagonal) e-ray optical data of Pitman et al. (2008; Figure 6 b). Specifically, the wavelength of peak polarisation and the profile shapes of both the polarisation and optical depth more closely follow the observations.

That the SiC polarisation signature dominates over that of silicates is testament to its stronger refractive indices and band

strength, i.e., absorption cross section per unit volume. In at least the crystalline samples this is accentuated by a polarisation reversal across the strong resonance (Martin 1975; Hong & Greenberg 1978), which essentially subtracts polarisation from the amorphous silicate at 10 μm.

In the interests of completeness, we computed models with SiC as a confocal mantle on a silicate core. These did not provide anywhere near as good a match to the observed optical depth and polarisation profiles. Similarly, models using the optical data of amorphous thin films of SiC from Mutschke et al. (1999) and Larruquert et al. (2011) did not match the spectra, being either too broad and/or peaking at the wrong wavelength. Given their weaker refractive indices than for the crystalline phases they also necessitated a larger relative abundance of SiC (compared to silicates). Finally, we replaced the 'astronomical silicate' with a magnesium-iron laboratory olivine, $Mg_{0.8}Fe_{1.2}SiO_4$, from Dorschner et al. (1995), motivated by its good match to the diffuse ISM MIR polarisation profile presented in Wright et al. (2002) and Wright & Glasse (2005). This provided very similar fits to the data.

In summary, both the conventional and polarisation spectra require the presence of a material with optical properties much like SiC, inclusive of a high band strength, a central wavelength near 11.3 μm and full width of a few microns. We thus assess the carrier of the additional absorption from approximately 10 to 12 μm in SVS13 to be SiC itself. But given the variation in the optical properties of specific types of SiC found in the literature a reliable estimate of its abundance is difficult. This is apart from a general statement that it is higher than in any other young star envelope or disc of which we know.

4.1.3 Crystalline silicates

The *ISO* crystalline silicate revolution (Jäger et al. 1998) came about because the *ISO* satellite was equipped with instruments capable of making measurements at longer wavelengths, where crystalline silicate features are not overwhelmed by those of more abundant and warmer amorphous silicates, as is usually the case in the *N*-band (Molster et al. 2010). There are three plausible mechanisms adept at producing crystalline silicates.

1. *Evaporation and re-condensation* Under high temperature and pressure condition in the immediate vicinity of the central star (< 1 au), dust grains can be evaporated and then re-condense as crystals (e.g., Grossman 1972).
2. *Thermal annealing* There have been at least three probable heat sources suggested in circumstellar discs [accretion luminosity in the inner region (∼1 au), Gail (2004); shock heating at a few au, Harker & Desch (2002); and disc surface layer annealing during accretion outburst, Ábrahám et al. (2009)]. Whatever the actual heat source(s) may be, the essence of the mechanism is simple annealing (i.e., heating of amorphous silicates and subsequent cooling to re-order the lattice structure).
3. *Low-temperature crystallisation* Put forward by Yamamoto and co-workers (e.g., Yamamoto & Chigai 2005), provided that an amorphous silicate core is coated with an organic (carbonaceous) refractory layer (Kimura, Mann & Jessberger 2003), a chemical reaction can be triggered at a low temperature (a few hundred K) to re-arrange the silicate lattice structure.

It is interesting to note that, so far, most detections of crystalline silicate features towards young stars have been in emission (e.g., Watson et al. 2009; Olofsson et al. 2009; Juhász et al. 2010), with only one recent report of clear detection of absorption (Poteet et al. 2011) to date,[5] a fact that may or may not favour one crystallisation mechanism over the others. Inclusions of the two most abundant crystalline silicate species, forsterite (Mg_2SiO_4) and enstatite ($MgSiO_3$), in absorption, substantially improve the model fitting in the current study. Equilibrium calculations suitable for the inner disc regions ($\lesssim$ 1 au, Gail 2004) show that these magnesium-rich crystalline silicates should dominate.

However, the crystalline silicate features are observed in absorption here and therefore the dust grains responsible for the signatures are likely to reside in the cold, outer regions. Apart from the low-temperature crystallisation described above, some means of heating is required to turn the amorphous lattice structure into crystalline, and if heating is only possible in the vicinity of the central star, an effective transport/mixing mechanism is required for crystalline silicates to be found in the remote, cooler regions. Indeed, crystalline silicates appear to be concentrated in the centre of many T-Tau systems, with more than 90 per cent of the 84 objects observed by Watson et al. (2009) showing strong 10-μm crystalline silicate features but only about 50 per cent having detectable 20−38-μm signatures, most probably indicating the temperature range of the crystalline silicates ($T \sim 200$ K at $\lesssim$ a few au, Watson et al. 2009). Olofsson et al. (2009), who, as part of the *Spitzer* cores-to-discs legacy programme, observed 108 young stars (66 of which were known T-Tau stars), identified what they termed the 'crystallinity paradox', wherein they found the cold crystalline features at wavelengths > 20 μm more frequently than those at ∼10 μm. However, when they re-examined it by analysing a further 58 *Spitzer* IRS spectra, they found a simultaneous enhancement of crystallinity in both the inner, warm and outer, cold regions (Olofsson et al. 2010). Sargent et al. (2009b) also reported comparable crystalline silicate abundances in the inner and outer disc regions in a *Spitzer* IRS study of 65 T-Tau stars. Although details may differ slightly, an undisputed universal outcome of all these investigations is the existence of processed (i.e., crystalline) materials in the outer, cooler parts of the circumstellar environment, as well as in the warmer, inner regions in the vicinity of the central star.

Comets contain crystalline silicates (e.g., Comet Hale-Bopp, Crovisier et al. 1996; 1997). The most definitive confirmation was once again found in the Stardust sample return from Comet 81P/Wild 2, the crystalline silicate mass fraction of which was as high as ∼0.5−0.65 (Westphal et al. 2009). The 81P/Wild 2 specimens also included chondrule-like particles (Nakamura et al. 2008), a clear indication that materials that constitute the comet experienced high temperatures in the past. Another clue to the apparent heating episode(s) in the Stardust samples is the presence of Calcium-, Aluminium-rich Inclusion (CAI)-like grains (Zolensky et al. 2006). However, as mentioned in §4.1.2, 81P/Wild 2 belongs to the short-period JFCs, which are believed to originate in the Kuiper Belt, extending from the orbit of Neptune (at ∼30 au) to approximately 50 au, in which the surface temperature of the most famous of its resident, Pluto, is only ∼40 K (Stern, Weintraub & Festou 1993).

[5] A tentative identification has been made for deeply embedded low-mass protostars IRAS 03445+3242 and HH46 IRS (Boogert et al. 2004), and for the high-mass YSO AFGL2591 (Aitken et al. 1988). Crystalline silicate absorption features towards other types of objects, e.g., ultra-luminous infrared galaxies (Spoon et al. 2006), have also been reported.

To overcome these facts at odds with each other (existence of high-temperature phases in cold regions), a number of mechanisms have been proposed to mix/transport radially the dust grains transformed near the central star. These include: the bipolar outflow 'X-wind' model (e.g., Shu, Shang & Lee 1996), accretion disc turbulence (e.g., Gail 2001; Bockelée-Morvan et al. 2002), spiral arms in marginally gravitationally unstable discs (e.g., Boss 2004), and outward transport in the disc mid-plane (e.g., Keller & Gail 2004; Ciesla 2007). Now, both chondrules and CAIs are sizable entities that often measure hundreds of μm and some as large as mm (chondrules) or even cm (CAIs) in diameter (e.g., Scott & Krot 2005; MacPherson et al. 2005). Although particles that large in the 81P/Wild 2 capture are rare (Hörz et al. 2006; Burchell et al. 2008), analogous to chondritic meteorites that contain large chondrules and CAIs, a similar size distribution may also be expected to exist in their probable natal bodies such as comets (Meier 2014). A recent modelling effort (Hughes & Armitage 2010) has found that particles of the size of chondrules and CAIs (a few mm or larger) cannot easily be transported out to the comet-forming region, regardless of their initial location. If this is the case, an in-situ production of melted grains[6] may have to be invoked. We will come back to this point in §4.2.

4.1.4 Annealed SiO_2

Aforementioned equilibrium calculations also show that, when the Mg/Si abundance ratio is $\lesssim 1$ (or perhaps after a significant amount of Mg has been taken up by forming forsterite), SiO_2 (and enstatite) becomes a major condensate (Ferrarotti & Gail 2001). Fabian et al. (2000) found that when they annealed enstatite ($MgSiO_3$) smoke at 1,000 K for 30 hours, the end product consisted of crystalline forsterite (Mg_2SiO_4), tridymite (crystalline SiO_2) and amorphous silica (SiO_2). This is a case similar to that reported by Bowen & Andersen (1914), who cooled a mixture of composition $MgSiO_3$ from the liquid state and found that, first forsterite separated out and, after further cooling, a mixture of silica and enstatite condensed. As crystalline silicates also exist, it may be deduced that some form of heating has melted $MgSiO_3$ and decomposed it into Mg_2SiO_4 and SiO_2. We further speculate that, once again, taking the presence of crystalline forsterite and enstatite as evidence, the cooling rate is just so that it would allow re-ordering of lattice structures to produce annealed SiO_2. Or, that crystalline SiO_2 is dominant over its amorphous counterpart in the stages immediately after their formation.

As mentioned earlier, SiO_2 has been identified in the MIR spectra of some young stars. Honda et al. (2003) observed a T-Tauri star Hen 3-600A in the *N*-band and their best-fit model included α-quartz (i.e., a type of crystalline SiO_2, from Spitzer & Kleinman 1961). Sargent et al. (2006) used optical constants of α-quartz from Wenrich & Christensen (1996) to analyse *N*-band spectra of 12 T-Tau stars. They found a small amount (up to a few per cent by mass) of crystalline SiO_2 in about a half of the objects studied. Amorphous silica (Henning & Mutschke 1997) and silica-rich glass (Koike et al. 1989) emissivities were ruled out by Sargent et al. (2009a), this time observing 5 more, different T-Tau stars, but inclusion of annealed SiO_2 (Fabian et al. 2000) gave a better fit. A *Spitzer* IRS spectrum of a β-Pictoris analogous (i.e., debris-disc) star HD172555, which suggested the presence of amorphous silica and SiO gas, was examined by Lisse et al. (2009). The 12.6-μm feature that would have indicated the existence of crystalline silica was not detected. They proposed planetesimal-scale (~km-size) hyper-velocity (> 10 km s^{-1}) impacts as the mechanism that produced fine (amorphous) silica dust and SiO gas. More recently, Fujiwara et al. (2012) obtained a *Spitzer* IRS spectrum of another debris-disc star HD15407A and concluded that incorporating an almost equal amount of fused (i.e., amorphous) quartz (Koike et al. 1989) and annealed silica (Fabian et al. 2000) provided the most satisfactory fit. They also favoured a similar scenario to that adopted by Lisse et al. (2009) for HD172555.

Although the number of samples is rather limited and most studies mentioned above did not set out specifically to probe crystalline or otherwise of silica dust structure, overall it is tempting to conclude that younger stars (T-Tauri stars, $\lesssim 10$ Myr) are more likely to possess more crystalline than amorphous SiO_2, while with slightly more evolved sources (debris-disc bearing stars, $\gtrsim 10$ Myr), the balance is tipped in the other direction. Also, if hyper-velocity planetesimal impacts are indeed required for the production of amorphous silica, this alone points to the latter stages in the evolution of protoplanetary discs. If this scenario is correct, then the natural implication may be that the circumstellar environment of (still deeply embedded and therefore much younger) PMS star SVS13 should contain mostly crystalline SiO_2 but not much (if at all) of its amorphous sibling.

4.2 Possible crystallisation mechanism and planet formation

We have demonstrated that crystalline silicates (forsterite and enstatite) and annealed SiO_2 exist in the cold, outer regions of circumstellar environment of the PMS star SVS13. Although we did not directly detect larger chondrules and CAIs in the current study, they may exist if the typical dust size distribution in chondritic meteorites also holds in the remote, cooler regions (at least in the comet-forming region at a few tens of au from the central star). If that is the case, an in-situ transformation mechanism of dust grains is probably required.

The runaway growth of planetesimals is the 'standard' model for terrestrial planet formation (e.g., Raymond et al. 2014). Outer gas giants, like Jupiter and Saturn, can be formed in a similar fashion via what is called the core-accretion (CA) model (e.g., Helled et al. 2014). But also feasible is if the remote, cold regions of the protoplanetary disc become gravitationally unstable and fragment, forming self-gravitating clumps, some of which will ultimately become gas giants (see e.g., Helled et al. 2014 and references therein).

According to the latter mechanism, commonly referred to as the disc instability (DI) model, fragmentation can take place at $\gtrsim 50$ au and clumps ranging from a few to ~10 M_J (Jupiter masses) may form (e.g., Boley et al. 2010; Forgan & Rice 2011; Rogers & Wadsley 2012). As these massive clumps contract and migrate inwards, the internal temperature rises and it can reach $\gtrsim 1{,}000$ K, sufficient to produce crystalline silicates, chondrules and CAIs (and dissolving amorphous carbon coating on SiC grains) *in situ*. When they are tidally disrupted, these thermally altered particles may be distributed at a wide range of radii to be re-captured by, e.g., comets (Vorobyov 2011; Nayakshin, Cha & Bridges 2011).

Of course, thermal processing of dust species can still occur in the immediate vicinity of the central star and the dust grains may be transported out to the comet-forming region of the pro-

[6] Note that grains in question here are not crystalline silicates so the low-temperature crystallisation of Yamamoto and co-workers mentioned earlier would not apply.

toplanetary disc. One of the plausible dust heating processes that could produce chondrules and CAIs (and at the same time a possible transport/mixing mechanism), is the X-wind model of Shu et al. (i.e., jets near the central star). But this has been criticised by Desch et al. (2010), who prefer shock-heating, due to DI but at a few au (e.g., Desch & Connolly 2002; see also Desch et al. 2012). However, as mentioned in §4.1.3, it is difficult, if not impossible, to move large particles such as chondrules and CAIs out to the comet-forming region, wherever their initial location may have been (Hughes & Armitage 2010). Even if shocks can be triggered, the gas density at the distance of the Kuiper Belt ($\gtrsim$ 30 au) is such that chondrule formation by shock-heating might not be feasible. Iida, Nakamoto & Susa (2001) estimate the pre-shock density of at least $10^{14.5}$ cm^{-3} is required, while both the minimum-mass Solar Nebula model of Hayashi (1981) and the minimum-mass extra-Solar nebula of Chiang & Laughlin (2013) predict a much lower density of the order $\sim 10^{10-11}$ cm^{-3} at 30 au.

We recall that SVS13 is a close binary, with a separation of $\sim$0.3 arcsec $\approx$ 71 au. Theory and model simulations depict some common features in the early stages of binary evolution: three separate discs (individual circumstellar discs around each component of the binary system and a circumbinary disc) and a clearing between the two classes of discs (e.g., Artymowicz & Lubow 1994; Bate & Bonnell 1997; Günther & Kley 2002). Under certain conditions, however, one binary component (primary) will gain a large circumstellar disc, while the other (secondary) only a small one (or none at all), with little to no circumbinary disc (Bate & Bonnell 1997). The primary is usually the dominant dust continuum source in PMS binary/multiple systems (e.g., Harris et al. 2012), and apart from a few outstanding cases, circumbinary discs appear to be elusive (Monin et al. 2007; Harris et al. 2012). In the case of SVS13, only one member of the binary (VLA 4B) exhibits significant dust emission (Anglada et al. 2004) and just a single object has been found in the NIR (which Hodapp & Chini 2014 identify as VLA 4B) as we do here in the MIR. Furthermore, the unresolved radio source exhibits a larger flux density than the sum of the resolved individual binary components, implying the existence of an extended envelope (Anglada et al. 2004). Also commonly seen in snapshots from simulations are spiral arms in all three discs due to the tidal interactions of the central binary. Whether such gravitational interplay and structures inhibit or enhance DI-induced fragmentation is a matter of debate (Mayer, Boss & Nelson 2010).

The 'clearing' or a gap between the circumbinary and the central circumstellar discs is also a product of the tidal interactions between the binary components, as the protoplanetary discs are stripped of materials and truncated to substantially smaller sizes compared to those around single stars (e.g., Artymowicz & Lubow 1994). Indeed, Anglada et al. (2004) found a compact structure at the position of VLA 4B of radius $\sim$30 au, clearly smaller than that often measured for discs around single stars of $\gtrsim$ 100 au (see e.g., Williams & Cieza 2011 and references therein). Discs are not only truncated but, in such a dynamic environment, they are also rapidly dispersed within a short period of time ($\lesssim$ 1 Myr), considerably shorter than a characteristic disc lifetime of $\gtrsim$ 2.5 Myr normally expected for single stars (e.g., Mamajek 2009), though the effect could be slightly milder for a binary separation of $\sim$70 au for SVS13 (Monin et al. 2007; Cieza et al. 2009). Although this type of disruptive impact might be thought to affect the planet formation negatively, Bonavita & Desidera (2007; see also Bonavita, Desidera & Gratton 2010) concluded that the detection frequencies of planets in single and binary systems are statistically identical. Most interestingly, Duchêne (2010) showed that, while binaries with separation wider than 100 au are indistinguishable from single stars in terms of trends regarding their protoplanetary discs, debris discs, and planets, close binaries in the range from 5 to 100 au exclusively host giant planets (i.e., those with mass $\gtrsim$ 1 M_J), or exhibit a distinct lack of planets smaller than 1 M_J. The two modes of planet formation discussed earlier present notably different timescales: CA with $\gtrsim$ a few Myr and DI $\lesssim$ 1 Myr (Helled et al. 2014). Considering the short lifetime of circumstellar discs in close binaries, it could be the case that DI is the only effective means of forming planets in them, and if so, the finding of Duchêne (2010) might just be a natural consequence of this.

Recent observations of the young low-mass binary system GG Tau A (Beck et al. 2012) have revealed that a 'streamer' of dust and gas, originating from the circumbinary disc and feeding the inner circumstellar discs can shock-excite H_2 gas at the interface, where the gas temperature was found to be in excess of 1,500 K. Unlike the shock-heating of particles (due to DI) rejected earlier because of the low density in the outer parts of the circumstellar disc, we surmise that a stream of material from the circumbinary disc piling up at the outer rim of the protoplanetary disc, combined with a higher shock velocity generated by streamers (20–30 km s^{-1} for streamers vs. $<$ 10 km s^{-1} for DI, Desch & Connolly 2002; Harker & Desch 2002; Beck et al. 2012), could make this a viable mechanism for melting/annealing dust grains *in situ* in the remote regions of circumstellar discs.

We therefore suggest that, amongst the processes that are capable of thermally altering dust grains, an in-situ mechanism is favoured for SVS13. Furthermore, the DI model for giant planet formation – provided that fragmentation occurs in circumstellar discs in binary systems – along with the shock-heating mechanism detected by Beck et al. (2012), is the leading candidate for producing crystalline silicates (and chondrules & CAIs), annealing SiO_2, as well as possibly dissolving the feature-concealing amorphous carbon layer from the SiC core. It remains to be seen if the scenarios just presented are rare or only occur in a short-lived evolutionary phase in shaping the distinctive *N*-band spectrum of SVS13. To this end, we are embarking on the search for similar objects and at the same time, it is hoped that work both in the laboratories and theoretical studies will advance sufficiently in the near future to solve, for example, the missing SiC problem.

5 CONCLUSIONS

The *N*-band spectrum of the low-mass PMS close binary system SVS13 is presented. The unique and complex spectrum is best modelled by a mixture of amorphous silicates, crystalline forsterite, crystalline enstatite, annealed SiO_2, and, most intriguingly of all, SiC, which has never before been identified in the circumstellar environment of a young star. The requirement for the inclusion of silicon carbide is also affirmed from the MIR polarimetry perspective. All these signatures are seen in absorption, implying the dust particles reside in remote, cold regions of the circumstellar environment. Speculation is made on possible origins of the dust species, especially those that have been processed and altered thermally, namely crystalline silicates and annealed SiO_2. The DI-induced fragmentation and the subsequent contraction and disruption of the giant planet embryos, along with the newly discovered shock-heating mechanism at the interface between the circumbinary and circumstellar discs, may be able to modify those dust grains *in situ* in the outer, cooler parts of the circumstellar environment. The heating

episode(s) provided by one or both of these processes can also feasibly reveal the hidden SiC feature.

ACKNOWLEDGEMENTS

Part of this work was conducted while TF was a Visiting Fellow at School of Physical, Environmental and Mathematical Sciences, UNSW Canberra, Australia. TF would like to thank their warm hospitality during his stay. CMW acknowledges support from the Australian Research Council Future Fellowship FT100100495. We would also like to thank the referee, Dr. Angela Speck, for her valuable comments.

REFERENCES

Ábrahám P., et al., 2009, Nature, 459, 224
Aitken D. K., 1989, in Kaldeich B. H., ed., Proc. 22nd ESLAB Symposium on Infrared Spectroscopy in Astronomy. ESA, p.99
Aitken D. K., 1996, in Roberge W. G., Whittet D. C. B., eds, Polarimetry of the Interstellar Medium. ASP Conf. Ser., Vol. 97, San Francisco, p.225
Aitken D. K., Roche P. F., Spenser P. M., Jones B., 1979, ApJ, 233, 925
Aitken D. K., Roche P. F., Smith C. H., James, S. D., Hough, J. H., 1988, MNRAS, 230, 629
Aitken D. K., Wright C. M., Smith C. H., Roche P. F., 1993, MNRAS, 262, 456
Anglada G., Rodríguez L. F., Torrelles J. M., 2000, ApJ, 542, L123
Anglada G., Rodríguez L. F., Osorio M., Torrelles J. M., Estalella R., Beltrán M. T., Ho P. T. P., 2004, ApJ, 605, L137
Artymowicz P., Lubow S. H., 1994, ApJ, 421, 651
Aspin C., 2003, AJ, 125, 1480
Aspin C., Sandell G., 1994, A&A, 288, 803
Bachiller R., Gueth F., Guilloteau S., Tafalla M., Dutrey A., 2000, A&A, 362, L33
Bate M. R., Bonnell I. A., 1997, MNRAS, 285, 33
Beck T. L., Bary J. S., Dutrey A., Piétu V., Guilloteau S., Lubow S. H., Simon M., 2012, ApJ, 754, 72
Bernatowicz T., Fraundorf G., Ming T., Anders E., Wopenka B., Zinner E., Fraundorf P., 1987, Nature, 330, 728
Bernatowicz T. J., Cowsik R., Gibbons P. C., Lodders K., Fegley B. Jr., Amari S., Lewis Roy S., 1996, ApJ, 472, 760
Bernatowicz T. J., Messenger S., Pravdivtseva O., Swan P., Walker R. M., 2003, Geochim. Cosmochim. Acta, 67, 4679
Bertie J. E., Labbé H.J., Whalley E., 1969, J. Chem. Phys., 50, 4501
Biscaya A. M., Rieke G. H., Narayanan G., Luhman K. L., Young E. T., 1997, ApJ, 419, 359
Blanco, A., Orofino V., Bussoletti E., Fonti S., Colangeli L., Stephens J. R., 1991, in Levasseur-Regourd A. C., Hasegawa H., eds, Origin and Evolution of Interplanetary Dust. Proc. IAU Colloq. 126, p.125
Blum R. D., Sellgren K., Depoy D. L., 1996, AJ, 112, 1988
Blum R. D., Ramírez S. V., Sellgren K., Olsen K., 2003, ApJ, 597, 323
Bockelée-Morvan D., Gautier D., Hersant F., Huré J.-M., Robert F., 2002, A&A, 384, 1107
Bohren C. F., Huffman D. R., 1983, Absorption and Scattering of Light by Small Particles. Wiley, New York
Boley A. C., Hayfield, T., Mayer L., Durisen R. H., 2010, ApJ, 695, L53
Bonavita M., Desidera S., 2007, A&A, 468, 721
Bonavita M., Desidera S., Gratton R., 2010, in Goździewski K., Niedzielski A., Schneider J., eds, Extrasolar planets in multi-body systems: theory and observations. EAS Publ. Ser., Vol.42, p.105
Boogert A. C. A., et al., 2004, ApJS, 154, 359
Boogert A. C. A., et al., 2008, ApJ, 678, 985
Boss A. P., 2004, ApJ, 616, 1265
Bowen N. L., Andersen O., 1914, Am. J. Sci., Series 4, 37, 487
Bradley J. P., 2003, in Davis A. M., ed., Treatise on Geochemistry Vol.1. Elsevier, Amsterdam, p. 689
Burchell M. J., et al., 2008, Meteoritics and Planet. Sci., 43, 23
Campins H., Ryan E. V., 1989, ApJ, 341, 1059
Carr J. S., 1989, ApJ, 345, 522
Carr J. S., Tokunaga A. T., Najita J., 2004, ApJ, 603, 213
Charnoz S., Morbidelli A., 2007, Icarus, 188, 468
Chiang E., Laughlin G., 2013, MNRAS, 431, 3444
Chiang E., Youdin A. N., 2010, Ann. Rev. Earth and Planet. Sci., 38, 493
Chigai T., Yamamoto T., 2003, Geochim. Cosmochim. Acta Supp., 67, 64
Choyke W. J., Palik E. D., 1985, in Palik E. D., ed., Handbook of Optical Constants of Solids. Academic Press, p.587
Chrysostomou A., Hough J. H., Messinger D. W., Whittet D. C. B., Aitken D. K., Roche P. F., 1996, in Roberge W. G., Whittet D. C. B., eds, Polarimetry of the Interstellar Medium. ASP Conf. Ser., Vol. 97, San Francisco, p.243
Ciesla F. J., 2007, Science, 318, 613
Cieza L. A., et al., 2009, ApJ, 696, L84
Clément D., Mutschke H., Klein R., Henning Th., 2003, ApJ, 594, 642
Clénet Y., Rouan D., Gendron E., Montri J., Rigaut F., Léna P., Lacombe F., 2001, A&A, 376, 124
Cohen M., Schwartz R. D., 1983, ApJ, 265, 877
Cohen M., Walker R. G., Carter B., Hammersley P., Kidger M., Noguchi K., 1999, AJ, 117, 1864
Cox P., 1989, A&A, 225, L1
Croat T. K., Stadermann F. J., 2006, Lunar and Planet. Sci. Conf., 37, 2048
Croat T. K., Stadermann F. J., 2008, Lunar and Planet. Sci. Conf., 39, 1739
Croat T. K., Stadermann F. J., Bernatowicz T. J., 2008, Meteoritics and Planet. Sci., 43, 1497
Croat T. K., Bernatowicz T. J., Stadermann F. J., 2009a, Lunar and Planet. Sci. Conf., 40, 1887
Croat T. K., Jadhav M., Lebsack E., Bernatowicz T. J., 2009b, Lunar and Planet. Sci. Conf., 40, 2175
Croat T. K., Stadermann F. J., Bernatowicz T. J., 2010a, Meteoritics and Planet. Sci. Supp., 73, 5327
Croat T. K., Stadermann F. J., Bernatowicz T. J., 2010b, AJ, 139, 2159
Croat T. K., Lebsack E., Bernatowicz T. J., 2010c, Lunar and Planet. Sci. Conf., 41, 1891
Croat T. K., Bernatowicz T. J., Jadhav M., 2014, Lunar and Planet. Sci. Conf., 45, 1441
Crovisier J., et al., 1996, A&A, 315, L385
Crovisier J., Leech K., Bockelee-Morvan D., Brooke T. Y., Hanner M. S., Altieri B., Keller H. U., Lellouch E., 1997, Science, 275, 1904
Davidson J., et al., 2009, Lunar and Planet. Sci. Conf., 40, 1853

Desch S. J., Connolly H. C. Jr., 2002, Meteoritics and Planet. Sci., 37,183
Desch S. J., Morris M. A., Connolly H. C. Jr., Boss A. P., 2010, ApJ, 725, 692
Desch S. J., Morris M. A., Connolly H. C., Boss A. P., 2012, Meteoritics and Planet. Sci., 47, 1139
Dorschner J., Begemann B., Henning Th., Jäger C., Mutschke H., 1995, A&A, 300, 503
Draine, B. T., 2003, ApJ, 598, 1026
Draine B. T., Allaf-Akbari, K., 2006, ApJ, 652, 1318
Draine B. T., Lee H. M., 1984, ApJ, 285, 89
Duchêne G., 2010, ApJ, 709, L114
Dwek E., Scalo J. M., 1980, ApJ, 239, 193
Eislöffel J., Günther E., Hessman F. V., Mundt R., Poetzel R., Carr J. S., Beckwith S., Ray T. P., 1991, ApJ, 383, L19
Fabian D., Jäger C., Henning Th., Dorschner J., Mutschke H., 2000, A&A, 364, 282
Ferrarotti A. S., Gail H.-P., 2001, A&A, 371, 133
Floss C., Stadermann F. J., Kearsley A. T., Burchell M. J., Ong W. J., 2013, ApJ, 763, 140
Forrest W. J., Gillett F. C., Stein W. A., 1975, ApJ, 195, 423
Frenklach M., Carmer C. S., Feigelson E. D., 1989, Nature, 339, 196
Forgan D., Rice K., 2011, MNRAS, 417, 1928
Fujiwara H., Onaka T., Yamashita T., Ishihara D., Kataza H., Fukagawa M., Takeda Y., Murakami H., 2012, ApJ, 749, L29
Gail H.-P., 2001, A&A, 378, 192
Gail H.-P., 2004, A&A, 413, 571
Gibb E. L., Whittet D. C. B., Boogert A. C. A., Tielens A. G. G. M., 2004, ApJS, 151, 35
Gillett F. C., Forrest W. J., Merrill K. M., Soifer B. T., Capps R. W., 1975, ApJ, 200, 609
Grossman L., 1972, Geochim. Cosmochim. Acta, 36, 597
Günther R., Kley W., 2002, A&A, 387, 550
Harker D., Desch S., 2002, ApJ, 565, 109
Harris R. J., Andrews S. M., Wilner D. J., Kraus A. L., 2012, ApJ, 751, 115
Harvey P. M., Wilking B. A., Joy M., 1984, ApJ, 278, 156
Hayashi C., 1981, Supplement to the Progress of Theoretical Physics, 70, 35
Helled R., et al., 2014 (to appear in Beuther H., Klessen R., Dullemond C., Henning Th., eds, Protostars and planets vi. Univ. Arizona Press)
Henning T., Mutschke H., 1997, A&A, 327, 743
Hildebrand R. H., Dragovan M., 1995, ApJ, 450, 663
Hodapp K. W., Chini R., 2014, arXiv:1408.5940v1
Holloway R. P., Chrysostomou A., Aitken D. K., Hough J.H., McCall A., 2002, MNRAS, 336, 425
Honda M., Kataza H., Okamoto Y. K., Miyata T., Yamashita T., Sako, S., Takubo S., Onaka T., 2003, ApJ, 585, L59
Hong S. S., Greenberg J. M., 1978, A&A, 69, 341
Hony S., Waters L. B. F. M., Tielens A. G. G. M., 2002, A&A, 390, 533
Horita T., et al., 2008, PASJ, 60, 37
Hörz F., et al., 2006, Science, 314, 1716
Hughes A. L. H., Armitage P. J., 2010, ApJ, 719, 1633
Hynes K. M., Croat T. K., Bernatowicz T. J., 2007, Lunar and Planet. Sci. Conf., 38, 1693
Iida A., Nakamoto T., Susa H., 2001, Icarus, 153, 430
Jäger C., Molster F. J., Dorschner J., Henning Th., Mutschke H., Waters L. B. F. M., 1998, A&A, 339, 904
Jones A. P., Nuth J. A. iii, 2011, A&A, 530, 44
Jones A. P., Tielens A. G. G. M., 1994, in Montmerle T., Lada C. L., Mirabel I. F., Tran Thanh Van J., eds, The cold universe. Gif-sur-Yvette, p.35
Jones A. P., Tielens A. G. G. M., Hollenbach D. J., McKee C. F., 1994, ApJ, 433, 797
Jones A. P., Tielens A. G. G. M., Hollenbach D. J., 1996, ApJ, 469, 740
Juhász A., et al., 2010, ApJ, 721, 431
Justtanont K., Yamamura I., de Jong T., Waters L. B. F. M., 1997, Ap&SS, 251, 25
Kataza H., Okamoto Y., Takubo S., Onaka T., Sako S., Nakamura K., Miyata T., Yamashita T., 2000, in Iye M., Moorwood A. F., eds, Optical and IR Telescope Instrumentation and Detectors. Proc. SPIE, 4008, 1144
Keller Ch., Gail H.-P., 2004, A&A, 415, 1177
Kemper F., Vriend W. J., Tielens A. G. G. M., 2004, ApJ, 609, 826
Kimura H., Mann I., Jessberger E. K., 2003, ApJ, 583, 314
Kimura Y., Saito Y., Kaito C., 2003, Surf. Sci., 527, L219
Koike C., Komatuzaki T., Hasegawa H., Asada N., 1989, MNRAS, 239, 127
Koike C., Imai Y., Chihara H., Suto H., Murata K., Tsuchiyama A., Tachibana S., Ohara S., 2010, ApJ, 709, 983
Kozasa T., Dorschner J., Henning T., Stognienko R., 1996, A&A, 307, 551
Kriss G., 1994, in Crabtree D. R., Hanisch R. J., Barnes J., eds, Astronomical Data Analysis Software and Systems iii. ASP Conf. Ser., Vol. 61, San Francisco, p.437
Laor A., Draine B. T., 1993, ApJ, 402, 441
Larruquert J. I., Pérez-Marín A. P., García-Cortés S., Rodríguez-de Marcos L., Aznárez J. A., Méndez J. A., 2011, J. Opt. Soc. America A, Vol.28, Issue 11, 2340
Lee H. M., Draine B. T., 1985, ApJ, 290, 211
Leger A., Gauthier S., Defourneau D., Rouan D., 1983, A&A, 117, 164
Levison H. F., Morbidelli A., Van Laerhoven C., Gomes R., Tsiganis K., 2008, Icarus, 196, 258
Li A., Draine B. T., 2002, ApJ, 564, 803
Liseau R., Lorenzetti D., Molinari S., 1992, A&A, 253, 119
Lisse C. M., Chen C. H., Wyatt M. C., Morlok A., Song I., Bryden G., Sheehan P., 2009, ApJ, 701, 2019
Lodders, K., Fegley B. Jr., 1995, Meteoritics, 30, 661
MacPherson G. J., Simon S. B., Davis A. M., Grossman L., Krot A. N., 2005, in Krot A. N., Scott E. R. D., Reipurth B., eds, Chondrites and the Protoplanetary Disk. ASP Conf. Ser. Vol.341, San Francisco, p.225
Maldoni M. M., Smith R. G., Robinson G., Rookyard V. L., 1998, MNRAS, 298, 251
Mamajek E. E., 2009, in Usuda, T., Ishii M, Tamura M., eds, Exoplanets and disks: their formation and diversity. AIP Conf. Proc., Vol.1158, p.3
Martin P. G., 1975, ApJ, 202, 393
Mayer L., Boss A., Nelson A. F., 2010, in Haghighpour N., ed., Planets in binary star systems. Ap&SS Lib., 366, 195
Meier M. M. M., 2014, Lunar and Planet. Institute Contrib. Ser., 1800, 5009
Mendybaev R. A., Beckett J. R., Grossman L., Stolper E., Cooper R. F., Bradley J. P., 2002, Geochim. Cosmochim. Acta, 66, 661
Messenger S., Joswiak D., Ito M., Matrajt G., Brownlee D. E., 2009, Lunar and Planet. Sci. Conf., 40, 1790
Min M., Waters L. B. F. M., de Koter A., Hovenier J. W., Keller L. P., Markwick-Kemper F., 2007, A&A, 462, 667

Molinari S., Liseau R., Lorenzetti D., 1993, A&AS, 101, 59
Molster F. J., Waters L. B. F. M., Kemper F., 2010, in Henning Th. ed., Astromineralogy. Springer, Berlin, p.143
Monin J.-L., Clarke C. J., Prato L., McCabe C., 2007, in Reipurth B., Jewitt D., Keil K., eds., Protostars and planets v. Univ. Arizona Press, Tucson, p.951
Mukai T., Koike C., 1990, Icarus, 87, 180
Mutschke H., Andersen A. C., Clément D., Henning Th., Peiter G., 1999, A&A, 345, 187
Nakamura T., et al., 2008, Science, 321, 1664
Nayakshin S., Cha S.-H., Bridges J. C., 2011, MNRAS, 416, L50
Olofsson J., et al., 2009, A&A, 507, 327
Olofsson J., Augereau J.-C., van Dishoeck E. F., Merín B., Grosso N., Ménard F., Blake G. A., Monin J.-L., 2010, A&A, 528, A39
Orofino V., Blanco A., Fonti S., 1994, A&A, 282, 657
Ott T., Eckart A., Genzel R., 1999, ApJ, 523, 248
Papoular R., 2008, MNRAS, 388, 457
Parise B., Simon T., Caux E., Dartois E., Ceccarelli C., Rayner J., Tielens A. G. G. M., 2003, A&A, 410, 897
Pegourie B., 1988, A&A, 194, 335
Pitman K. M., Hofmeister A. M., Corman A. B., Speck A. K., 2008, A&A, 483, 661
Poppe T., 2003, Icarus, 164, 139
Posch Th., Mutschke H., Andersen A., 2004, ApJ, 616, 1167
Poteet C. A., et al., 2011, ApJ, 733, L32
Raymond S. N., Kokubo E., Morbidelli A., Morishima R., Walsh K. J., 2014 (to appear in Beuther H., Klessen R., Dullemond C., Henning Th., eds, Protostars and planets vi. Univ. Arizona Press)
Roberge A., Feldman P. D., Weinberger A. J., Deleuil M., Bouret J.-C., 2006, Nature, 441, 724
Robinson G., Smith R. G., Maldoni M. M., 2012, MNRAS, 424, 1530
Roche P. F, Aitken D. K., 1985, MNRAS, 215, 425
Rodríguez L. F., Anglada G., Curiel S. 1997, ApJ, 480, L125
Rogers P. D., Wadsley J., 2012, MNRAS, 423, 1896
Roskosz M., Gillot J., Capet F., Roussel P., Leroux H., 2011, A&A, 529, 111
Sargent B. A., et al., 2006, ApJ, 645, 395
Sargent B. A., et al., 2009a, ApJ, 690, 1193
Sargent B. A., et al., 2009b, ApJS, 182, 477
Scott E. R. D., Krot A. N., 2005, in Krot A. N., Scott E. R. D., Reipurth B., eds, Chondrites and the Protoplanetary Disk. ASP Conf. Ser. Vol.341, San Francisco, p.15
Shu F. H., Shang H., Lee T., 1996, Science, 271, 1545
Smith C. H., Wright C. M., Aitken D. K., Roche P. F., Hough J. H., 2000, MNRAS, 312, 327
Smith R. G., Sellgren K., Tokunaga A. T., 1989, ApJ, 344, 413
Smith R. G., Wright C. M., 2011, MNRAS, 414, 3764
Somsikov V. V., Voshchinnikov N. V., 1999, A&A, 345, 315
Speck A. K., Barlow M. J., Skinner C. J., 1997, MNRAS, 288, 431
Speck A. K., Thompson G. D., Hofmeister A. M., 2005, ApJ, 634, 426
Spitzer W. G., Kleinman D. A., 1961, Phys. Rev., 121, 1324
Spoon H. W. W. et al., 2006, ApJ, 638, 759
Stern S. A., Weintraub D. A., Festou M. C., 1993, Science, 261, 1713
Strom S. E., Vrba F. J., Strom K. M., 1976, AJ, 81, 314
Tamanai A., Mutschke H., Blum J., Meeus G., 2006, ApJ, 648, L147
Thronson H. A. Jr., 1979, A&A, 75, 236
Treffers R., Cohen M., 1974, ApJ, 188, 545
Vorobyov E. I., 2011, ApJ, 728, L45
Watson D. M., et al., 2009, ApJS, 180, 84
Weidenschilling S. J., 2000, Space Sci. Rev., 92, 295
Weingartner J. C., Draine B. T., 2001, ApJ, 548, 296
Wenrich M. L., Christensen P. R., 1996, J. Geophys. Res., 101, 15921
Westphal A. J., Fakra S. C., Gainsforth Z., Marcus M. A., Ogliore R. C., Butterworth A. L., 2009, ApJ, 694, 18
Whittet D. C. B., 2003, Dust in the Galactic Environment. IOP Publishing, London
Whittet D. C. B., Duley W. W., Martin P. G., 1990, MNRAS, 244, 427
Williams P. J., Cieza L. A., 2011, ARA&A, 49, 67
Wright C. M., Glasse A. C. H., 2005, in Adamson A., Aspin C., Davis C. J., Fujiyoshi T., eds, Astronomical Polarimetry: Current Status and Future Directions. ASP Conf. Ser., Vol.343, San Francisco, p.316
Wright C. M., Aitken D. K., Smith C. H., Roche P. F., 1999, in Greenberg J. M., Li A., eds, Formation and Evolution of Solids in Space. Kluwer, Dordrecht, p.77
Wright C. M., Aitken D. K., Smith C. H., Roche P. F., Laureijs R. J., 2002, in Alves J. F., McCaughrean M. J., eds, The Origin of Stars and Planets: the VLT View. Springer-Verlag, p.85
Wright C. M., Siebenmorgen R., Stecklum B., Sterzik M., Kaufl H.-U., 2008, in McLean I. S., Casali M. M., eds, Ground-based and Airborne Instrumentation for Astronomy ii. Proc. SPIE, 7014, 701429
Yamamoto T., Chigai T., 2005, Highlights of Astronomy, 13, 522
Yasuda Y., Kozasa T., 2012, ApJ, 745, 159
Zhang K., Jiang B. W., Li A., 2009, MNRAS, 396, 1247
Zinner E., 1998, Ann. Rev. Planet. Sci., 26, 147
Zolensky M. E., et al., 2006, Science, 314, 1735